

Christina A. Pedersen · Jan-Gunnar Winther

Intercomparison and validation of snow albedo parameterization schemes in climate models

Received: 12 August 2004 / Accepted: 26 April 2005 / Published online: 15 July 2005
© Springer-Verlag 2005

Abstract Snow albedo is known to be crucial for heat exchange at high latitudes and high altitudes, and is also an important parameter in General Circulation Models (GCMs) because of its strong positive feedback properties. In this study, seven GCM snow albedo schemes and a multiple linear regression model were intercompared and validated against 59 years of in situ data from Svalbard, the French Alps and six stations in the former Soviet Union. For each site, the significant meteorological parameters for modeling the snow albedo were identified by constructing the 95% confidence intervals. The significant parameters were found to be: temperature, snow depth, positive degree day and a dummy of snow depth, and the multiple linear regression model was constructed to include these. Overall, the intercomparison showed that the modeled snow albedo varied more than the observed albedo for all models, and that the albedo was often underestimated. In addition, for several of the models, the snow albedo decreased at a faster rate or by a greater magnitude during the winter snow metamorphosis than the observed albedo. Both the temperature dependent schemes and the prognostic schemes showed shortcomings.

1 Introduction

Snow, with its high albedo, is known to be crucial for heat exchange at high latitudes and high altitudes, and it is an important parameter in General Circulation Models (GCMs) because of its strong positive feedback properties. A warmer climate leads to a reduction of snow extent followed by a decrease in wintertime land surface albedo (Houghton et al. 2001). This can create a

positive feedback mechanism where the amount of radiation absorbed is increased, leading to further warming.

The classical model works of Wiscombe and Warren (1980), Warren and Wiscombe (1980) and Warren (1982) thoroughly discuss the various factors affecting the albedo, such as snow depth, grain size, liquid water content, solar incident angle and contamination (Hansen and Nazarenko 2003). Albedo is wavelength dependent, and the albedo at a particular wavelength λ is defined as (Perovich et al. 2002):

$$\alpha(\lambda) = \frac{F_{\uparrow}(\lambda)}{F_{\downarrow}(\lambda)}, \quad (1)$$

where F_{\uparrow} and F_{\downarrow} is the spectral reflected and incident shortwave irradiance, respectively. The wavelength-integrated, or total albedo, α_t , is found from integrating the fluxes on the right-hand side of Eq. 1 over the solar spectrum.

Current snow and sea-ice albedo parameterizations are highly simplistic, but over the last two decades, substantial knowledge of the reflective characteristics of snow, glaciers, and sea ice has been gained, and a wide variety of field measurements (Grenfell and Perovich 2004; Aoki et al. 2003; Winther et al. 2003; Gerland et al. 1999; Perovich et al. 2002; Ivanov 1999; Oerlemans and Knap 1998; Perovich et al. 1998; Betts and Ball 1997; Baker et al. 1991; Winther et al. 1999) and theoretical studies (Brock et al. 2000; Gerland et al. 2000; Roesch 2000; Sergent et al. 1993; Winther 1993; Baker et al. 1990; Marshall 1989; Winther et al. 2002) have been reported. Therefore, it seems timely to utilize this detailed knowledge to improve the parameterization of snow albedo in climate models. Some snow modeling studies, where albedo was one of the investigated parameters, have already been subjected to comparisons (Essery et al. 1999; Jin et al. 1999; Boone and Etchevers, 2001; Aoki et al. 2003; Yang et al. 1997; Slater et al. 1998), but these comparisons included relatively few models which were validated against in situ data from a few sites.

C. A. Pedersen (✉) · J.-G. Winther
Norwegian Polar Institute, 9296, Tromsø, Norway
E-mail: christina@npolar.no

The snow albedo models that include the snow cover fractions are presented in Sect. 2; while in Sect. 3 the data from Svalbard, the French Alps and six sites in the former Soviet Union is described. In Sect. 4, the multiple linear regression model is introduced, together with some background theory. The main results and the discussion are presented in Sect. 5 and the conclusions in Sect. 6.

2 The GCM snow albedo models

The General Circulation Models (GCMs) are computationally very expensive, so in general, only very simple albedo parameterizations are used. In this study the albedo schemes were examined in an uncoupled system, and no feedback effects were considered. Where the model parameterizations included forest fraction, leaf area index or surface slopes, these were ignored.

2.1 Snow albedo schemes

The seven GCM snow albedo models, summarized in Table 1, were divided into two categories depending on the model complexity. The temperature dependent category, which included ECHAM5 (Roeckner et al. 2003) and UKMO (Essery et al. 2001; Essery et al. 1999), had the simplest scheme with a temperature dependent snow albedo, which varied linearly between a minimum value at the melting point and a maximum value for cold temperatures. Above and below these limits the albedo was fixed. The surface albedo was a weighed value between the snow and ground albedo according to the snow depth.

The prognostic albedo category consisted of all the other models: ECMWF (Internet Page 2003), CLASS (Verseghy 1991), ISBA (Douville et al. 1995), GISS (Hansen et al. 1983) and BATS (Bonan et al. 2002). The three models ECMWF, CLASS and ISBA had a prognostic albedo scheme, i.e., the snow albedo value at a time step was dependent on the snow albedo value at the previous time step. The models had different decay factors with time for melting and non-melting snow. GISS had a prognostic procedure for snow age, where the albedo was an exponential function of the age. These models had the albedo value reset to its maximum value for new snowfall above a certain precipitation threshold. The surface albedo was weighted according to the snow cover fraction, between the snow and bare ground albedo. BATS had different parameterizations for the visible and near-infrared band, and also for diffuse and direct radiation, but the datasets used in this work lacked this information, and BATS was reduced to a prognostic albedo model for snow age, similar to the ones given above. Again, the surface albedo was a weighted mean dependent on the snow depth. The snow cover fraction we used in BATS was not the one originally included in the model (Bonan et al. 2002), but the

one introduced by Yang et al. (1997) to avoid the bias due to underestimated snow cover fraction.

2.2 Snow cover fraction

The snow cover fraction plays an important role in the total surface albedo, because if the snow cover fraction is underestimated then the surface albedo will be also (Roesch et al. 2001). The snow cover fraction parameterizations are given in Table 1 and illustrated in Fig. 1. As can be seen, the snow cover fractions show the same characteristics, with steep and sharp curves, but with individual differences in the growth rate. At a snow depth of 2.5 cm, the snow cover fractions vary between 0.4 (CLASS) to 0.89 (ISBA), while at a depth of 10 cm, the fractions are above 0.9 for all the models. ISBA has the fastest increase, while CLASS increases slowest for shallow depths. Most of the models reach 1.0 for deep snow depths. The parameterizations are in agreement with the results from Baker et al. (1991), which showed two distinct stages for the relationship between albedo and snow depths, where the surface albedo increased sharply as the snow depth increased until it reached a critical depth, after which, the surface albedo increased slowly as the depth increased.

3 In situ validation data

The snow albedo models were validated against in situ measurements from Ny-Ålesund, Svalbard, Col de Porte in the French Alps and six stations in the former Soviet Union (Fig. 2). These datasets were collected at point sites, in contrast to the models which have a spatial resolution on the scale of hundreds of km, and therefore the assumption that the albedo and meteorological data were representative of a specified grid square was made.

In Table 2 a summary of the sites and the available meteorological parameters are presented. The data from Ny-Ålesund at 78.9°N 11.9°E was collected during the years 1981–2002. The polar night, where the whole of the Sun remains below the sea-level horizon, starts 25 October and ends 17 February. Ny-Ålesund experiences cold winters and summers and receives low amounts of precipitation. Net shortwave radiation was determined by means of two Kipp & Zonen pyranometers over the wavelength band 305–2800 nm (Hisdal et al. 1992; Hisdal and Finnekåsa 1996). Hourly albedo values were calculated when the global radiation was above a certain threshold, and daily values were calculated based on a mean of hourly values.

The data from Col de Porte in the northern French Alps, located 1340 m above sea level at 45.3°N 5.8°E was collected during the years 1993–1996. The average air temperature at Col de Porte is about 0°C during the winter months, and the precipitation received is high relative to Ny-Ålesund. The incoming and reflected shortwave radiation were measured with an Eppley

Table 1 Albedo parameterization schemes included in our comparison. T_s is the surface temperature and θ_0 the solar zenith angle. The snow depth is given as S_n in snow water equivalent and d_s in m

Centre	Model/Reference	Snow Albedo	Snow Cover Fraction
Max Planck Institute for Meteorology	ECHAM5 Roehner et al. (2003)	Temperature dependent: Linear function of T_s between -5°C and 0°C . Fixed above 0°C at $\alpha_{\min} = 0.3$ and below -5°C at $\alpha_{\max} = 0.8$.	Tanh function of S_n and slope terrain.
Hadley Centre and UK Meteorological Office Forecast model	UKMO Essery et al. (2001, 1999)	Temperature dependent: Linear function of T_s between -2°C and 0°C . Fixed above 0°C at $\alpha_{\min} = 0.5$ and below -2°C at $\alpha_{\max} = 0.8$.	Exponentially decaying function of S_n .
European Centre for Medium-Range Weather Forecasts	ECMWF Web page (2003)	Prognostic procedure: Non-melt: constant decay Melt: exponential decay Reset to $\alpha_{\max} = 0.85$ at large snowfall.	Linear function of S_n for $S_n < 0.015\text{m}$. 1.0 elsewhere.
Canadian Climate Centre	CLASS Verseghy (1991)	Prognostic procedure: Different exponential decay for T_s above/below 0°C . Reset to $\alpha_{\max} = 0.84$ at large snowfalls.	Linear function of S_n and inverse proportional to the snow density.
Météo France	ARPEGE with ISBA Land-Surface Scheme Douville et al. (1995)	Prognostic procedure: Cold snow: constant decay Melting snow: exponential decay Reset to $\alpha_{\max} = 0.85$ at large snowfalls.	Non-linear function of S_n .
Goddard Institute for Space Studies	GISS Hansen et al. (1983)	Exponentially decaying function of snow age, where the snow age is a prognostic function, exponential dependent of new snow fall. Reset to $\alpha_{\max} = 0.85$ at large snowfalls.	Exponentially decaying function of S_n .
National Center for Atmospheric Research	BATS Bonan et al. (2002)	Linear dependence on snow age and non-linear dependence on θ_0 . Snow age is a function of change in S_n .	Tanh function of d_s (approach suggested by Yang et al. 1997).

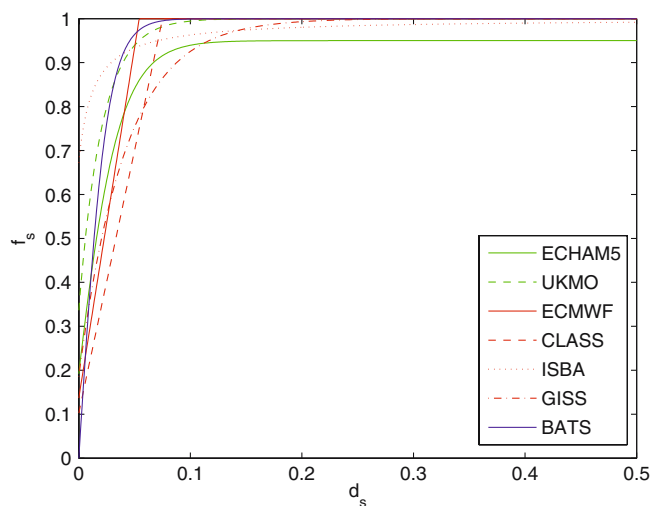


Fig. 1 Snow cover fraction (f_s) as a function of snow depth (d_s) in [m] for the albedo models. For CLASS a constant density of 200 kg/m^3 was used in this figure

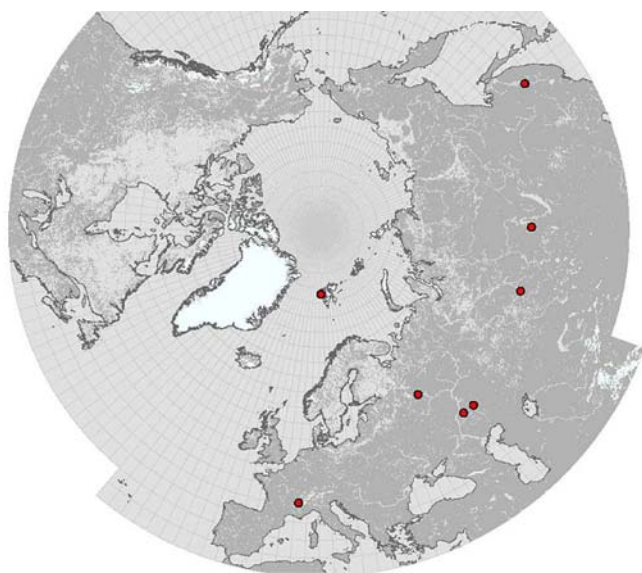


Fig. 2 The in situ validation sites

Table 2 The available meteorological parameters from each validation site is marked with an X. C means corrected measurement, while R is raw data. Est. is used when the snow depth is estimated instead of being measured directly

Parameter	Ny-Ålesund	Col de Porte	FSU Stations
Surface albedo	X	X	X
Air temp.	X	X	X
Surface temp.			X
Max&min temp.	X		
Wind speed	X	X	X
Precipitation	X(R)	X(C)	X(R)
Precip. type		X	
Cloud cover Fr.	X	X	X
Snow depth	Est.	X	Est.

pyranometer over the wavelength band 280–2800 nm (Lejeune and Martin 1995). Daily albedo data was obtained by dividing the total reflected by the total incoming shortwave radiation received during the day. Only the hours where the incoming shortwave radiation was greater than 10 W/m^2 and the snow depth was above 10 cm were considered. In this way, this dataset differs from the others since no data for snow depths below 10 cm exists. The snow pack at Col de Porte was affected by leaves from the trees, which influenced the albedo values (P. Etchevers, private communication, 2004). The leaves darkened the snow and lowered the albedo by about 10–15% compared to the clean snow case (P. Etchevers, private communication, 2004). The dataset from this site has been used for validation of UKMO, ISBA and two hydrological and avalanche models (Essery et al. 1999).

Datasets from six soil stations localized in the former Soviet Union (FSU) for the period 1978–1983 were also included (Robock et al. 2000). The stations were part of the Hydrometeorological Service in the former Soviet Union described by Vinnikov and Yeserkepova (1991) and include Khabarovsk at 48.5°N 135.2°E , Kostroma at 57.8°N 41.0°E , Ogurtsovo at 54.9°N 83.0°E , Tulun at 54.6°N 100.6°E , Uralsk at 51.3°N 51.4°E and Yershov at 51.4°N 48.3°E . The upward and downward shortwave radiation were measured by Yanishevsky Pyranometers over the wavelength band 300–2800 nm (K.Y. Vinnikov, private communication, 2004). The daily albedo values were a mean of the three-hourly values when the Sun angle was more than 20° above the horizon. The sun zenith angle was calculated according to Iqbal (1983), using algorithms from R. Storvold (private communication, 2004). The same dataset has been used in testing the BATS (Yang et al. 1997) and BASE (Slater et al. 1998) models.

Snow depth is not a standard measured parameter at regular meteorological stations, so to estimate the snow depth for the stations where it was missing, the hydrological model HBV (Swedish Meteorological and Hydrological Institute 2001) developed by the Swedish Meteorological and Hydrological Institute, was used. The HBV model is the standard forecasting tool used in Norway and Sweden, and operational and scientific applications of it are widely known. Only daily mean values of temperature and precipitation are required input for the model, and it calculates snow depth and free water content in the snow at a fixed point in time. The amount of water input into the HBV model is given by the precipitation, so the quality of the precipitation data is crucial (Killingtveit and Sæther 2001). However, it can almost always be assumed that measured precipitation is less than true precipitation (Hanssen-Bauer et al. 1996), and several correction procedures for different precipitation gauges exist (Førland et al. 1996; Hanssen-Bauer et al. 1996; Yang et al. 1997; Yang et al. 1995). The HBV model was tested with both uncorrected and corrected precipitation measurements from Ny-Ålesund for the years 1998–2000, and compared with

acoustic snow depth measurements from the same site (not shown). Surprisingly, it was shown that the HBV model with the uncorrected precipitation data corresponded better to the measured snow depths than the model with the corrected data, therefore the HBV model with uncorrected precipitation data was used in this study. The conversion between snow depth and snow water equivalent was calculated from Pomeroy and Gray (1995).

3.1 Climatology

The monthly mean surface albedo and its standard deviation are shown for all sites in Fig. 3. As can be seen, the monthly mean albedo differs greatly between the sites. The high Arctic site of Ny-Ålesund has the highest monthly albedo with 0.86 in February and March, followed by values greater than 0.81 for April and May. None of the other sites have such high values. The FSU sites have the lowest winter albedo values, with values down to 0.65 for Khabarovsk in February. The spring and autumn transitions at all sites are characterized by large standard deviations in the albedo, with Ny-Ålesund having the highest.

The measured albedo at Col de Porte was 10–15% lower than it would be in the clean snow case due to darkening from leaves (P. Etchevers, private communication, 2004). Without this darkening, the albedo would be about the same as for Ny-Ålesund in February. In the cold winter months, we would expect the albedo values to be similar. For the rest of the winter, however, lower albedo values were expected, and observed at Col de Porte. The FSU stations showed substantially lower albedo values. These values were lower than the leaf-darkened Col de Porte values. The number of days with air temperature above -1°C was counted to investigate

if melting could explain the large deviations between Ny-Ålesund and the FSU sites, but it was found that Ny-Ålesund and the FSU sites had the same number of warm days (on average less than 3) in January and February. Col de Porte, on the other hand, experienced more than 10 warm days on average in January and February. Also the winter snow depth plays an important role in the determination of the snow albedo. For some of the FSU stations, the low winter albedo values can be partly explained by the shallow snow pack (depth around 5–10 cm) for some of the years, which decreased the monthly average albedo to unusually low values. However, for the rest of the FSU sites such a clear correlation between the snow depth and the albedo value during the cold winter months could not be seen. We suspect that the different spectrometer used for albedo measurements can partly explain the difference in observed surface albedo. Also, possible contamination at the FSU sites may be an additional reason for this discrepancy.

4 Multiple linear regression analysis

The general form of a multiple linear regression model (MLRM) for k independent variables is given by (Montgomery et al. 2001):

$$\mathbf{y} = \mathbf{X}\mathbf{2}\beta + 2\epsilon. \quad (2)$$

In general \mathbf{y} is the observations, \mathbf{X} the matrix of regression variables, β the regression coefficients, and ϵ is the random errors (Montgomery et al. 2001). It is assumed that the error terms ϵ_i have $E(\epsilon_i)=0$ and $\text{Var}(\epsilon_i)=\sigma^2$, and that the error terms are uncorrelated. In this setup \mathbf{y} represents the albedo and \mathbf{X} is a matrix of available meteorological parameters.

If some of the meteorological parameters are linearly dependent (multicollinear) the least mean square estimate of β will suffer from large errors. Instead, β was estimated from ridge regression, where the ridge estimator $2\hat{\beta}_R$ is the biased estimator with smaller variance than the unbiased least mean square solution, and it is given by (Montgomery et al. 2001):

$$2\hat{\beta}_R = (\mathbf{X}'\mathbf{X} + b\mathbf{I})^{-1}\mathbf{X}'\mathbf{y}, \quad (3)$$

where $b \geq 0$ is a biasing parameter (constant). The bias in $2\hat{\beta}_R$ increases with b , while the variance decreases as b increases. b was chosen such that the reduction in the variance was greater than the increase in the bias, as (Montgomery et al. 2001):

$$b = \frac{k\hat{\sigma}^2}{2\hat{\beta}'_R 2\hat{\beta}_R}, \quad (4)$$

where $2\hat{\beta}_R$ and $\hat{\sigma}^2$ were found from the least mean square solution (Montgomery et al. 2001), and k is the number of regressors.

The building of the multiple linear regression model by including only a subset of the available meteorolog-

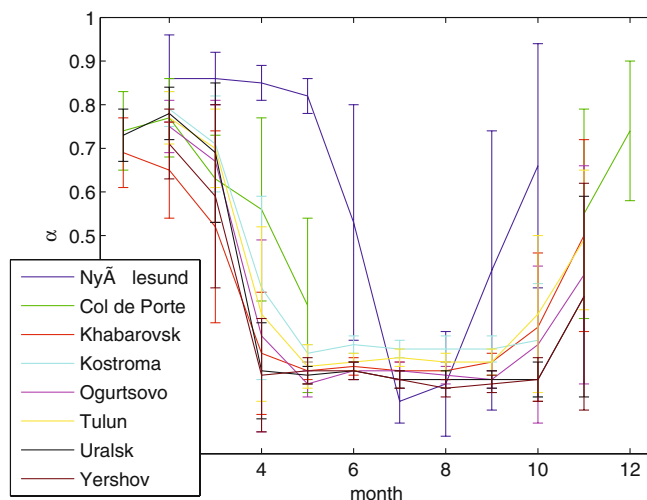


Fig. 3 Climatology of the monthly mean snow albedo and the standard deviation (as error bars) when snow is on the ground for the months

ical parameters involves a trade off between including as many parameters as possible, so that the information content is maintained, and including as few parameters as possible because the variance of the prediction value increases with the number of parameters used. So, the multiple linear regression model was built to include only the meteorological parameters that were of real value in explaining the albedo response. Thus, the significance of each meteorological parameter for modeling the snow albedo was tested by constructing the 95% confidence interval for each regressor coefficient as (Kleinbaum et al. 1988)

$$\hat{\beta}_j < t_{\alpha} \sqrt{\hat{\sigma}^2 C_{jj}} \quad (5)$$

where C_{jj} is the j -th diagonal element for the $(\mathbf{X}'\mathbf{X})^{-1}$ matrix, and $t_{\alpha} = t_{\alpha, n-k-1}$ is the quantile from the student t distribution with $n-k-1$ degrees of freedom, where n is the number of data points. If the regressor coefficient confidence interval includes zero, the coefficient is not significantly different from zero, and the corresponding meteorological parameter should not be included in the MLRM for snow albedo.

Positive accumulated degree days (i.e., a variable of accumulated positive temperatures since last snowfall), a dummy variable to indicate if snow is on the ground or not and an offset (constant) were included in the pool of candidate regressors. The positive accumulated degree days is a non-linear function of temperature, and therefore it makes sense to include both this parameter and the temperature. This parameter was also included in the regression models of Baker et al. (1990) and Brock et al. (2000).

It is crucial to test the MLRM on data not included in the building of the model (Montgomery et al. 2001). If not, the prediction error will be underestimated. To evaluate the prediction quality of the MLRM, the available data for each site was divided into two sets: one “training set” and one “test set”. All the data, except data from one year, was used to build the model (training set), and the data of the last year was used to test the predictive properties of the model (test set).

5 Results and discussion

The snow albedo MLRM was built by considering the following meteorological parameters: temperature, cloud cover, precipitation, wind speed, snow depth, positive degree day and dummy snow fall. In addition a constant was added. Only the days where the snow depth was above zero were included in the calculations. The regressor coefficients were calculated from ridge regression, and the 95% one-at-a-time confidence intervals for each regression coefficient are shown in Fig. 4. For Ny-Ålesund, the mean temperature, snow depth, positive degree day, dummy snowfall and constant were significant, for Col de Porte, the temperature, cloud cover, positive degree day, dummy snowfall and

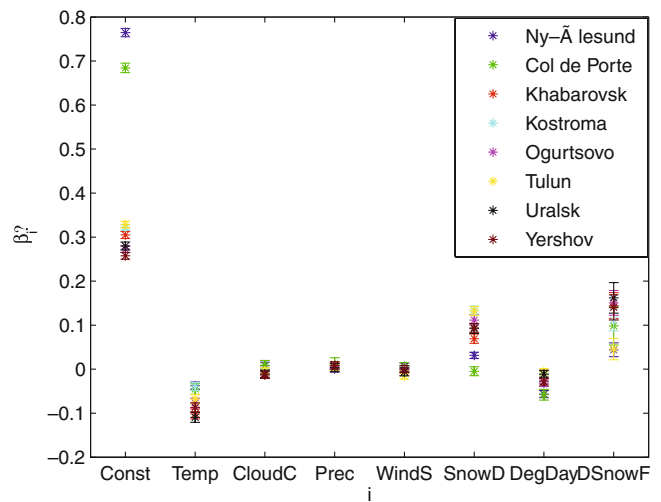


Fig. 4 The 95% one-at-a-time confidence interval for each meteorological parameter coefficient. The star gives the estimated regression coefficient, while the bars give the upper and lower limits of the confidence interval. The abbreviation used are the following: Const = constant, Temp = temperature, CloudC = cloud cover, Prec = precipitation, WindS = wind speed, SnowD = snow depth, DegDay = positive degree day and DSnowF = dummy snow fall

constant were significant, while for the FSU stations (on average) the temperature, cloud cover, snow depth, positive degree day, dummy snowfall and constant were significant (the results for the individual FSU stations are summarized in Table 3). The multiple linear regression model was built to only include the parameters shown to be significant in the snow albedo MLRM.

Snow depth proved not to be significant for Col de Porte, which was the only site where snow depth was measured and not calculated. The reason is probably that the snow albedo was measured only for days where the snow depth was above 10 cm. That is, the snow was “optically thick”, and the snow depth played only a minor role in the snow albedo determination. Marshall and Oglesby (1994) surmised that snow aging, grain size and temperature were relatively more important early in the melt season, while decreasing fractional snow cover (and thereby snow depth) appeared to be relatively more important during the middle and latter stages of snow melt.

5.1 General snow albedo model features

The GCMs and the MLRM were validated against 59 years of data from the eight sites. Based on the seasonal observed and modeled albedo, some generalizations were made. First, the observed snow albedo at Ny-Ålesund and Col de Porte attained very high values, above 0.95 for Ny-Ålesund and 0.90 for Col de Porte for new snow fall, which were well above what was given by any models (the maximum albedo threshold for any model was $\alpha_{\max} = 0.85$). For the six FSU sites the albedo

Table 3 The significant meteorological parameters in the MLRM. X is significant, and – is not significant. For precipitation, the first symbol is for uncorrected precipitation, while the latter is for the corrected. The abbreviations are the same as in Fig. 4

Site	Const	Temp	CloudC	Wind	Prec	SnowD	PosDegDay	DSnowF
Ny-Ålesund	X	X	–	–	–	X	X	X
Col de Porte	X	X	X	–	–	–	X	X
Khabarovsk	X	X	X	–	–/X	X	X	X
Kostroma	X	X	–	–	–/X	X	X	X
Ogurtsovo	X	X	X	–	–/–	X	X	X
Tulun	X	X	–	X	–/–	X	–	X
Uralsk	X	X	X	–	–/–	X	X	X
Yershov	X	X	X	–	–/X	X	X	X
All FSU	X	X	X	–	–	X	X	X

values were substantially lower, and the modeled values were closer to what was observed. Second, the modeled snow albedo varied more than the observed albedo for all models and sites. This was especially the case for Ny-Ålesund and Col de Porte, where the observed snow albedo stayed relatively high and constant through the whole cold winter. Third, the modeled snow albedo decreased at a faster rate or by a larger magnitude during the winter snow metamorphosis than the observed albedo. For Col de Porte, which was a temperate site where the snow melted and re-froze during the winter, some of the model albedos decreased rapidly during the melt.

During melt season, the modeled snow albedo was very dependent on the snow cover fraction, which again was determined almost entirely by the snow depth. All the models showed the same characteristics, which supports the interpretation that the spring albedo's main determinant was snow depth. For Col de Porte, where the snow depth was measured, the models responded accurately by decreasing the snow albedo at a correct rate and time. For the other sites, where the snow depth was calculated from the HBV model, the results were somewhat less satisfying. For Ny-Ålesund, the models had the spring decay just as often too early as delayed, while for the FSU stations the modeled snow albedo had a delayed spring decay. These changes were highly cor-

related with the degree of accuracy of the calculated snow depth. However, we found this characteristic for the FSU stations difficult to reconcile since the HBV snow depths were calculated based on uncorrected precipitation data. By correcting the data, the amount of precipitation would increase, leading to an increased winter snow cover (Hanssen-Bauer et al. 1996), which again leads to a delayed melt. So, if the corrected precipitation had been used in the HBV model, the bias would have increased.

5.2 Model type features

There were also important features connected with the models' categories, as shown in Fig. 5 and described below. The albedo time evolution of the two temperature dependent schemes, ECHAM5 and UKMO, are shown in the upper panel of Fig. 5a for Col de Porte in 1995. The lower panel shows the corresponding air temperature, where the horizontal lines give the 0°C, –2°C and –5°C temperature thresholds. The temperature dependent schemes showed a weakness by fixing the albedo to its minimum value ($\alpha_{\min}=0.3$ for ECHAM5 and $\alpha_{\min}=0.5$ for UKMO) when the temperature increased above 0°C. At a temperate site like Col de Porte, where the temperature was at 0°C several times during

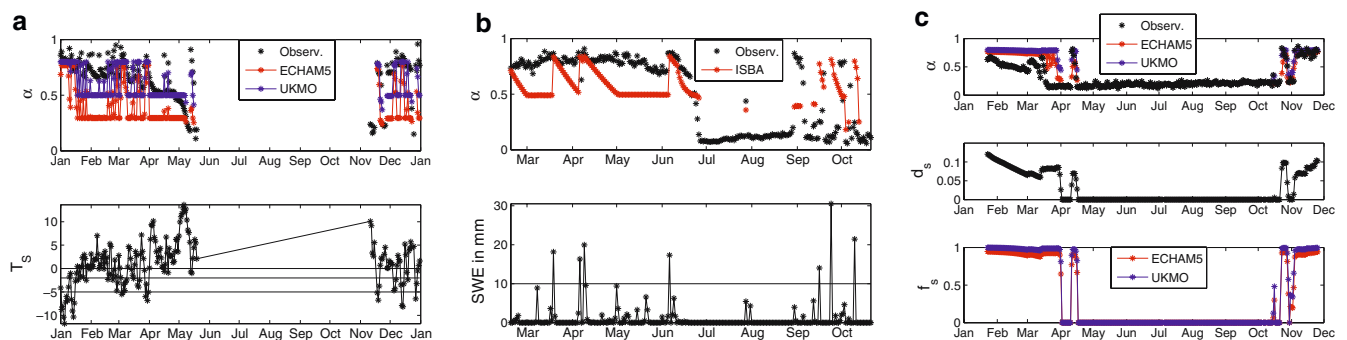


Fig. 5 Examples of model shortcomings from categories of snow albedo parameterization schemes. **a** shows the temperature dependent albedo schemes ECHAM5 and UKMO (upper panel) together with the surface temperature (lower panel) for Col de Porte in 1995. **b** shows the prognostic ISBA albedo scheme (upper panel) and the

reset of the snow albedo at large snow falls, together with daily snowfall in [mm] (lower panel) from Ny-Ålesund in 2000. **c** shows the snow albedo schemes (ECHAM5 and UKMO—upper panel) sensitivity to snow depth in [m] (middle panel) and snow cover fraction (lower panel) for Khabarovsk in 1981

the winter without the observed albedo dropping significantly, this feature became dominant and unrealistic. Also in the melting period, the temperature dependent schemes decreased the snow albedo too early and too fast.

In Fig. 5b the prognostic ISBA snow albedo scheme is shown together with the observed albedo for Ny-Ålesund in 2000 (upper panel). The snow albedo in the prognostic schemes decreases exponentially with snow age. The middle panel shows ISBA, where the snow albedo was fixed at its minimum value $\alpha_{\min} = 0.5$, until a new snowfall above a certain precipitation threshold occurred. The lower panel shows the precipitation, with the specified precipitation threshold for ISBA (10 mm SWE - shown as the horizontal black line). In a low precipitation site like Ny-Ålesund, a new snowfall above this threshold rarely happens, and the albedo is wrongly fixed at its minimum value for long periods. This shortcoming occurred for all the prognostic albedo schemes, but was predominant for ISBA because of its large precipitation threshold. The new snowfall threshold (precipitation threshold) varied among the models between 2–10 mm SWE. In addition, the precipitation measurements are connected with large uncertainties, and the determination of the threshold value can cause large errors.

Figure 5c shows the surface albedo dependency of snow cover fraction. The upper panel shows the observed seasonal albedo together with the model results from ECHAM5 and UKMO from Khabarovsk in 1981. The middle panel shows the snow depth, which is below 13 cm during the whole winter. However, the snow

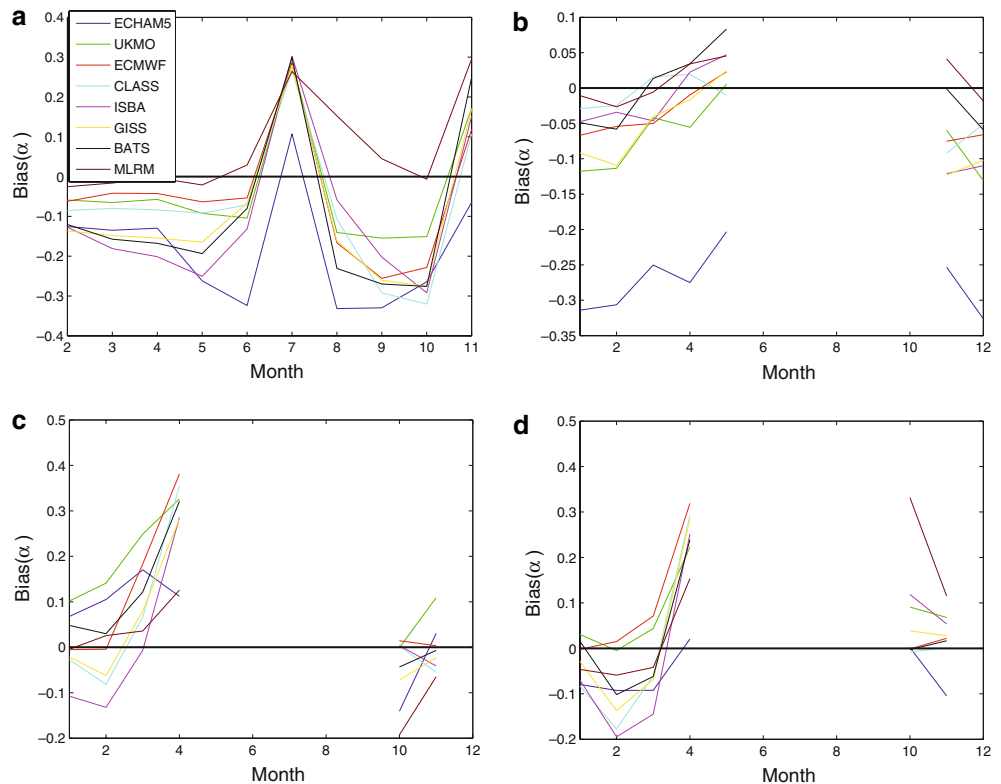
cover fraction parameterizations for the models show a snow cover fraction close to one (lower panel). It is clear that the models overestimate the albedo because of an overestimation of the snow cover fraction.

5.3 Objective validation of the snow albedo models

The monthly mean bias between the modeled and observed albedo is shown for four of the sites in Fig. 6a–d. Despite the differences in the models' snow albedo parameterizations all models show a similar bias pattern. For Ny-Ålesund in Fig. 6a, most of the models underestimated the albedo in the winter and autumn, but during snow melt in spring and snow accumulation in late autumn the models overestimated the albedo. The peaks should, however, be treated with caution, since they were based on very few observations (only the days where the snow depths were above zero were considered, and these were few in spring and autumn). The clear underestimation by all the models may indicate that the albedo values for Ny-Ålesund during the cold winter were unusually high. A similar pattern with the bias going from underestimation to overestimation (or smaller bias to higher bias) during the spring was also found for the other sites (Fig. 6b–d). The smallest bias was found for Col de Porte, where we know the albedo was lowered due to leaves on the ground. This indicates that the models underestimate the albedo.

The variance of the observed and modeled albedo are shown in Fig. 7a–d for the same four sites. The variance

Fig. 6 The monthly mean bias between the modeled and observed albedo in **a** Ny-Ålesund, **b** Col de Porte, **c** Khabarovsk and **d** Uralsk. Note the different scales of the plots



was lowest in the early, cold winter and increased, during the snow melting in spring. Loth et al. (1993) stated that an albedo change from 0.7 to 0.35 in 4 days is typical during melting periods, so large variances in spring are expected. A variance peak also occurred during snow accumulation in autumn. For Ny-Ålesund, the variance has an asymmetric shape, and it is clear that the spring melt proceeds at a more rapid rate than the autumn freezing. However, it is interesting that the variance of the modeled albedo was smaller or of the same size as the variance of the observed albedo for many of the models and sites. This is in contrast to the often unrealistic rapid and steep decay which was observed for some of the models during the winter snow metamorphose. The other FSU stations showed similar characteristics to Khabarovsk and Kostroma, and their figures were therefore omitted.

The root mean square errors (RMSE) and correlation coefficients (ρ) between observed and modeled albedo are given in Table 4. The RMSE measures the offset between the model and observations, while ρ measures the linear co-variance. Together these two measurements describe the goodness of the fit. The lowest RMSE (0.07) and highest ρ (0.79–0.80) were found for ECHAM5, BATS and MLRM for various sites. The MLRM had the smallest RMSE on average for all sites. There was a clear difference between the models' performance among the sites, with the models overall performing better for the FSU sites, because of their relative lower albedo measurements. The high RMSE for ECHAM5 in Ny-Ålesund and Col de Porte is explained earlier in con-

nection to Fig. 5a. The shallow snow cover at Tulun had the CLASS snow cover fraction, and thereby the CLASS albedo, underestimated, giving a high RMSE at 0.30. The corresponding low ρ at 0.06 occurred because of changing signs on ρ making the average close to 0. Also the relative low correlation coefficients between the models ISBA, GISS and CLASS and the observed albedo for the last four FSU stations were due to shallow snow covers and underestimated snow cover fractions. A scatterplot of RMSE against ρ is shown in Fig. 8. A “good” model is characterized by a small RMSE and a ρ close to 1.0, so the best models should be clustered in the upper left corner of the figure. Although some trends can be seen, the scatterplot shows no clear clustering of the models, and no model can be considered to be superior to all the others.

An unpaired t test to determine if the mean modeled and observed albedos were significantly different was performed, by testing the null hypothesis H_0 that the mean of the modeled albedo was equal to the mean of the observed albedo, against the alternative hypothesis H_1 that they were not equal. The sample test statistics were calculated according to Walpole et al. (2002). At a significance level of $\alpha=0.05$ the MLRM was the only model where the modeled albedo was equal to the observed albedo for all the sites. The CLASS model albedo was equal to the observed for two sites (Col de Porte and Khabarovsk), while the ECHAM5, BATS and ISBA model albedos were equal to the observed means for one site each. For all the other models the null hypothesis was rejected for all sites.

Fig. 7 The monthly mean variance of the modeled and observed albedo in **a** Ny-Ålesund, **b** Col de Porte, **c** Khabarovsk and **d** Uralsk. The variance of the observed albedo is colored in *gray*, while the model variances are shown by the *curves*. Note the different scales of the plots

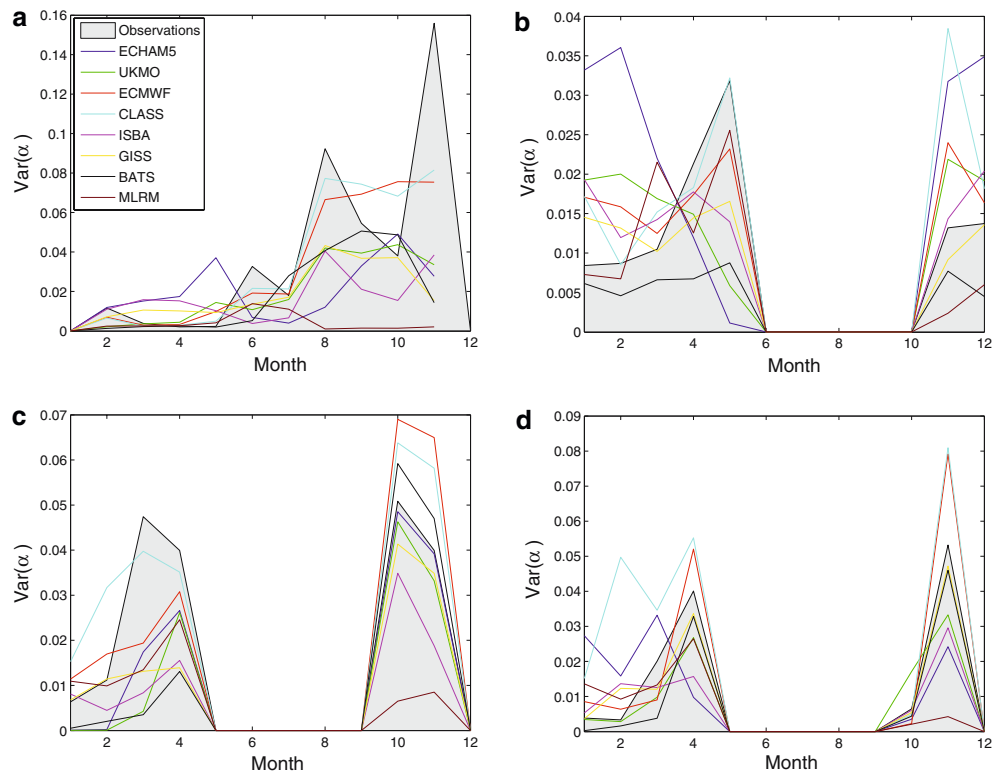


Table 4 Total average RMSE and ρ (in brackets) between the observed and modeled albedo. The mean RMSE and ρ are also given for each model

	ECHAM5	UKMO	ISBA	GISS	CLASS	ECMWF	BATS	MLRM
Ny-Ålesund	0.23 (0.48)	0.14 (0.52)	0.21 (0.33)	0.19 (0.43)	0.18 (0.45)	0.16 (0.47)	0.19 (0.41)	0.10 (0.55)
Col de Porte	0.31 (0.51)	0.14 (0.62)	0.11 (0.71)	0.11 (0.72)	0.09 (0.78)	0.10 (0.75)	0.08 (0.79)	0.08 (0.80)
Khabarovsk	0.11 (0.69)	0.14 (0.58)	0.11 (0.47)	0.10 (0.64)	0.12 (0.57)	0.14 (0.46)	0.11 (0.62)	0.10 (0.57)
Kostroma	0.09 (0.66)	0.08 (0.65)	0.08 (0.56)	0.08 (0.57)	0.10 (0.54)	0.10 (0.60)	0.07 (0.75)	0.07 (0.72)
Ogurtsovo	0.08 (0.75)	0.11 (0.63)	0.12 (0.19)	0.11 (0.44)	0.12 (0.47)	0.13 (0.40)	0.10 (0.51)	0.09 (0.66)
Tulun	0.07 (0.80)	0.10 (0.74)	0.12 (0.50)	0.11 (0.65)	0.30 (0.06)	0.11 (0.61)	0.08 (0.77)	0.09 (0.72)
Uralsk	0.09 (0.71)	0.08 (0.74)	0.12 (0.27)	0.11 (0.41)	0.14 (0.23)	0.10 (0.59)	0.09 (0.60)	0.09 (0.54)
Yershov	0.08 (0.74)	0.10 (0.74)	0.11 (0.35)	0.11 (0.47)	0.12 (0.47)	0.12 (0.62)	0.09 (0.60)	0.08 (0.70)
Mean	0.13 (0.67)	0.11 (0.65)	0.12 (0.42)	0.11 (0.54)	0.15 (0.45)	0.12 (0.56)	0.10 (0.63)	0.09 (0.66)

In order to further investigate the meaning of the correlation coefficient ρ , a single sample test of $H_0: \rho_{\text{obs},i} = \rho_{\text{obs},j}$ was performed, where $\rho_{\text{obs},i}$ ($\rho_{\text{obs},j}$) is the correlation between the observations and model i (j). That is, the correlation coefficient between the observed albedo and one model was compared to the correlation coefficient between the observed albedo and another model. The test statistic was computed according to Kleinbaum et al. (1988) using the sample correlations between observations and models and between models. For a large number of samples, the test statistic has approximately a standard normal distribution under H_0 (Kleinbaum et al. 1988). At a significance level of $\alpha = 0.05$ it was found that the null hypothesis had to be rejected for most of the model combinations, that is, the correlation coefficients were not equal. Some exceptions were that the correlation between ECHAM5 and UKMO (the two temperature dependent schemes) was found to be equal for three of the sites and the correlations between ISBA and GISS, CLASS and ECMWF and the correlations between MLRM and UKMO, CLASS and BATS were equal for two of the sites. A tendency is that the temperature dependent schemes

were similar to each other and the prognostic schemes were similar to each other.

6 Conclusions

The overall goal of this work was not to determine a single “best snow albedo parameterization scheme”. Instead the characteristics of the seven GCMs and the multiple linear regression model were investigated, and the models were intercompared with each other and with in situ validation data. Eight sites covering the northern hemisphere (Svalbard, the French Alps and six stations in the former Soviet Union) were used as validation data.

A multiple linear regression model was fit to the validation data, and the significant meteorological parameters for modeling the snow albedo were identified to include: temperature, a dummy of snow fall and a constant for all of the sites. In addition, for Ny-Ålesund snow depth and accumulated positive degree days were significant, for Col de Porte accumulated positive degree days and cloud cover were significant, while for the FSU stations, snow depth and cloud cover were significant. This means that when building a snow albedo model (whether it is in GCMs or elsewhere), these meteorological parameters should be included.

Large differences existed between the observed albedo in Ny-Ålesund and the former Soviet Union stations, with very high cold winter albedo values in Ny-Ålesund. The modeled snow albedo was more variable than the observed snow albedo for all models and sites, and the modeled albedo decreased at a faster rate or by a larger magnitude during the winter snow metamorphosis than the observed albedo. The snow albedo was also most often underestimated by the models. During snow melt, the modeled albedo was almost entirely determined by the snow cover fraction, i.e., snow depth, and an underestimated snow cover fraction led to an underestimated surface albedo, and vice versa. From the scatterplot of RMSE and the correlation coefficient, it was clear that none of the models was superior to the others for all sites.

The snow albedo schemes were divided into two categories: temperature dependent schemes and prog-

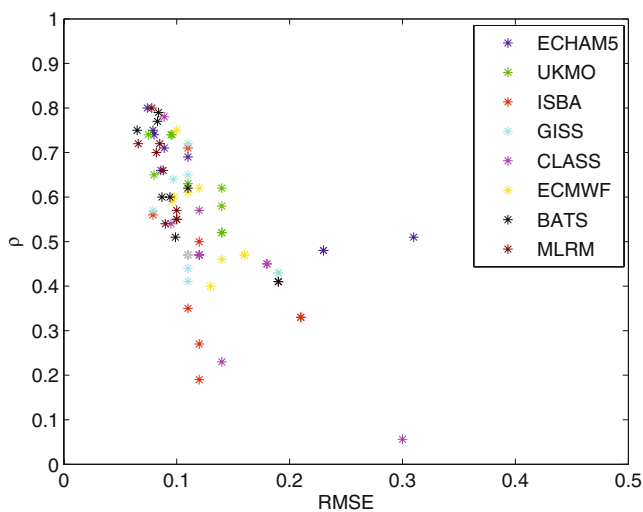


Fig. 8 Scatterplot of RMSE against ρ for all models. Each color represents a model for all sites. A “good” model is characterized by a small RMSE and a ρ close to one

nostic schemes. The temperature dependent schemes were too sensitive to temperatures, by fixing the albedo to its minimum value when the temperature exceeded freezing. We feel that the prognostic snow albedo schemes are superior to the temperature dependent schemes, but the new snowfall threshold, which varied widely among the models, needs to be more carefully examined.

More work remains to be done on the snow albedo parameterization. The intercomparison needs to be considered on a larger spatial scale, i.e., GCM grids. Other factors will then become important in the investigation, e.g., the snow cover fraction will be of special interest, and must be defined on a GCM grid. In situ ground validation data could be replaced with remote sensing validation data. For example, the Moderate Resolution Imaging Spectroradiometer (MODIS) snow albedo product is currently available, and could be a valuable data source in this context (Klein and Stroeve 2002).

Acknowledgements The work is supported by the Research Council of Norway, the Norwegian Polar Institute and the University of Tromsø. We thank J.-B. Ørbæk for providing data from Ny-Ålesund, P. Etchevers for providing data from Col de Porte, and A. Robock and N. Speranskaya for valuable information regarding the data from the former Soviet stations. Further, we acknowledge R. Essery, J. Hansen, E. Roeckner, D. Verseghy and Z.-L. Yang for answering questions regarding their respective GCM models and albedo parameterization, and G. Elvebakk for valuable discussions regarding the multiple linear regression model. We also would like to thank F. Godtlielsen, D. K. Hall, B. Ivanov, M. Költzow, A. Ohmura, E. Roeckner and A. C. Roesch for valuable comments during the early stage of the work, and R. Hall and P. Lewis are acknowledged for their careful review of the manuscript.

References

- Aoki T, Hachikubo A, Hori M (2003) Effects of snow physical parameters on shortwave broadband albedos. *J Geophys Res* 108(D19)
- Baker DG, Ruschy DL, Wall DB (1990) The albedo decay of prairie snows. *J Appl Meteorol – Notes and Correspondence* 29:179–187
- Baker DG, Skaggs RH, Ruschy DL (1991) Snow depth required to mask the underlying surface. *J Appl Meteorol – Notes and Correspondence* 30:387–392
- Betts AK, Ball JH (1997) Albedo over the Boreal Forest. *J Geophys Res* 102(D24):28901–28909
- Bonan GB, Oleson KW, Vertenstein M, Levis S, Zeng X, Dai Y, Dickinson RE, Yang Z-L (2002) The land surface climatology of the community land model coupled to the NCAR community climate Model. *J Climate* 15:3123–3149
- Boone A, Etchevers P (2001) An intercomparison of three snow schemes of varying complexity coupled to the same land surface model: local-scale evaluation at an alpine site. *J Hydrometeorol* 2:374–394
- Brock BW, Willis IC, Sharp MJ (2000) Measurement and parameterization of albedo variations at Haut Glacier d'Arolla, Switzerland. *J Glaciol* 46(155)
- Douville H, Royer J-F, Mahfouf J-F (1995) A new snow parameterization for the Météo France climate model. *Climate Dyn* 12:21–35
- Essery R, Martin E, Douville H, Fernández A, Brun E (1999) A comparison of four snow models using observations from an alpine site. *Climate Dyn* 15:583–593
- Essery R, Best M, Cox P (2001) MOSES 2.2 Technical documentation. Technical report, Hadley Centre, Met Office, UK
- Førland EJ, Allerup P, Dahlström B, Elomaa E, Jónsson T, Madsen H, Perälä J, Rissanen P, Vedin H, Vejen F (1996) Report No. 24/96: manual for operational correction of nordic precipitation data. Norwegian Meteorological Institute
- Gerland S, Winther J-G, Ørbæk JB, Liston GE, Øritsland NA, Blanco A, Ivanov B (1999) Physical and optical properties of snow covering arctic tundra on Svalbard. *Hydrol Process* 13:2331–2343
- Gerland S, Liston GE, Winther J-G, Ørbæk JB, Ivanov BV (2000) Attenuation of solar radiation in arctic snow: field observations and modelling. *Ann Glaciol* 31:364–368
- Grenfell T, Perovich DK (2004) Seasonal and spatial evolution of albedo in a snow-ice-land-ocean environment. *J Geophys Res* 109(C1)
- Hansen J, Nazarenko L (2003) Soot climate forcing via snow and ice albedos. *P Natl Acad Sci USA* 101(2):423–428
- Hansen J, Russell G, Rind D, Stone P, Lacis A, Lebedeff S, Ruedy R, Travis L (1983) Efficient three-dimensional global models for climate studies: model I and II. *Mon Weather Rev* 111(4):609–662
- Hanssen-Bauer I, Førland EJ, Nordli PØ (1996) Report No. 31/96: measured and true precipitation at Svalbard. Technical report, Norwegian Meteorological Institute
- Hisdal V, Finnekåsa Ø (1996) Radiation measurements in Ny-Ålesund, Spitsbergen 1988–1992. Technical report, Norwegian Polar Institute
- Hisdal V, Finnekåsa Ø, Vinje T (1992) Radiation measurements in Ny-Ålesund, Spitsbergen 1981–1987. Technical report, Norwegian Polar Institute
- Houghton JT, Ding Y, Griggs DJ, Noguer M, van der Linden PJ, Dai X, Maskell K, Johnson CA (eds) (2001) *Climate change 2001: the scientific basis*. Cambridge University Press
- Internet Page (2003) <http://www.ecmwf.int/research/ifsd/docs/physics/>. European Centre for Medium-Range Weather Forecasts
- Iqbal M (1983) *An introduction to solar radiation*. Academic Press, New York
- Ivanov BV (1999) New data on sea-ice Albedo in the Laptev and Barents Seas. In: Kassens H, Bauch HA, Dmitrenko I, Eicken H, Hubberten H-W, Melles M, Thiede J, Timokhov L (eds) *Land-ocean systems in the Siberian Arctic: dynamics and history*. Springer, Berlin Heidelberg New York, pp 59–63
- Jin J, Gao X, Yang Z-L, Bales RC, Sorooshian S, Dickinson RE, Sun SF, Wu GX (1999) Comparative analysis of physically based snowmelt models for climate simulations. *J Climate* 12:2643–2657
- Killingtveit Å, Sæther B (2001) Hydrologiske modeller for Tilsigsprognosering - Med Hovedvekt p HBV-modellen (in Norwegian)
- Klein AG, Stroeve J (2002) Development and validation of a snow albedo algorithm for the MODIS instrument. *Ann Glaciol* 34:45–52
- Kleinbaum DG, Kupper LL, Muller KE (1988) *Applied regression analysis and other multivariable methods*. Duxbury Press
- Lejeune Y, Martin E (1995) Application du Modele CROCUS aux Donnees de la Saison 93/94 du Col de Porte et de la Campagne Leadex 92 (in French). Technical Report No 6, Météo France
- Loth B, Graf H-F, Oberhuber JM (1993) Snow cover model for global climate simulations. *J Geophys Res* 98(D6):10451–10464
- Marshall SE (1989) A physical parameterization of snow albedo for use in climate models. PhD thesis, University of Washington, National Center for Atmospheric Research and University of Colorado
- Marshall S, Oglesby RJ (1994) An improved snow hydrology for GCMs. Part 1: snow cover fraction, albedo, grain size and age. *Climate Dyn* 10:21–37
- Montgomery DC, Peck EA, Vining GG (2001) *Introduction to linear regression analysis*. Wiley
- Oerlemans J, Knap WH (1998) A 1 year record of global radiation and albedo in the ablation zone of Morteratschgletscher, Switzerland. *J Glaciol* 44(147):231–238

- Perovich DK, Roesler CS, Pegau WS (1998) Variability in Arctic Sea ice optical properties. *J Geophys Res* 103(C1):1193–1208
- Perovich DK, Grenfell TC, Light B, Hobbs PV (2002) Seasonal evolution of the albedo of multiyear Arctic Sea ice. *J Geophys Res* 107(C10)
- Pomeroy JW, Gray DM (1995) Snowcover. Accumulation, relocation and management. NHRI Science Report No. 7
- Robock A, Vinnikov KY, Srinivasan G, Entin JK, Hollinger SE, Speranskaya NA, Liu S, Namkhai A (2000) The global soil moisture data bank. *Bull Am Meteorol Soc* 81(6):1281–1299
- Roeckner E, Bäuml G, Bonaventura L, Brokopf R, Esch M, Giorgetta M, Hagemann S, Kirchner I, Kornbluh L, Manzini E, Rhodin A, Schlese U, Schulzweida U, Tompkins A (2003) The atmospheric general circulation model ECHAM5 - part 1. Technical Report 349, Max Planck Institute for Meteorology
- Roesch AC (2000) Assessment of the land surface scheme in climate models with focus on surface albedo and snow cover. PhD thesis, Swiss Federal Institute of Technology Zurich
- Roesch A, Wild M, Gilgen H, Ohmura A (2001) A new snow cover fraction parameterisation for the ECHAM4 GCM. *Climate Dyn* 17:933–946
- Sergent C, Pougatch E, Sudul M, Bourdelles B (1993) Experimental investigation of optical snow properties. *Ann Glaciol* 17
- Slater AG, Pitman AJ, Desborough CE (1998) The validation of a snow parameterization designed for use in general circulation models. *Int J Climatol* 18:595–617
- Swedish Meteorological and Hydrological Institute (2001) HBV/IHMS-Information
- Verseghy DL (1991) CLASS - A Canadian land surface scheme for GCMs. I. Soil model. *Int J climatol* 11:111–133
- Vinnikov KY, Yeserkepova IB (1991) Soil moisture: empirical data and model results. *J Climate* 4:66–79
- Walpole RE, Myers RH, Myers SL, Ye K (2002) Probability and statistics for engineers and scientists. Prentice Hall
- Warren SG (1982) Optical properties of snow. *Rev Geophys Space Phys* 20(1):67–89
- Warren SG, Wiscombe WJ (1980) A model for the spectral albedo of snow. II: snow containing atmospheric aerosols. *J Atmos Sci* 37:2724–2745
- Winther J-G (1993) Short- and long-term variability of snow albedo. *Nordic Hydrol* 24:199–212
- Winther J-G, Gerland S, Ørbæk JB, Ivanov B, Blanco A, Boike J (1999) Spectral reflectance of melting snow in a high Arctic watershed on Svalbard: some implications for optical satellite remote sensing studies. *Hydrol Process* 13:2033–2049
- Winther J-G, Godtlielsen F, Gerland S, Isachsen PE (2002) Surface albedo in Ny-Ålesund, Svalbard: variability and trends during 1981–1997. *Global Planet Change* 32:127–139
- Winther J-G, Bruland O, Sand K, Gerland S, Marechal D, Ivanov B, Glowacki P, König M (2003) Snow research in Svalbard - an overview. *Polar Res* 22(2):125–144
- Wiscombe WJ, Warren SG (1980) A model for the spectral albedo of snow. I: pure snow. *J Atmos Sci* 37:2712–2733
- Yang D, Goodison BE, Metcalfe JR, Golubev VS, Elomaa E, Gunther T, Bates R, Pangburn T, Hanson CL, Emerson D, Copaciu V, Milkovic J (1995) Accuracy of Tretyakov precipitation gauge: result of WMO intercomparison. *Hydrol Process* 9:877–895
- Yang Z-L, Dickinson RE, Robock A, Vinnikov KY (1997) Validation of the snow submodel of the biosphere-atmosphere transfer scheme with Russian snow cover and meteorological observational data. *J Climate* 10:353–373